Applied Mathematics & Information Sciences
An International Journal

http://dx.doi.org/10.18576/amis/110335

A Comparative Study of Spectral Methods for Valuing Financial Options

Francis Youbi, Edson Pindza[*]*, and Eben Maré*

Department of Mathematics and Applied Mathematics, University of Pretoria, Pretoria 002, Republic of South Africa

Received: 12 Mar. 2017, Revised: 19 Apr. 2017, Accepted: 22 Apr. 2017
Published online: 1 May 2017

Abstract: Spectral methods have been actively developed in the last decades. The main advantage of these methods is that they yield exponential order accuracy if the function is smooth enough. However, for discontinuous functions, their accuracy deteriorates to low accuracy due to the Gibbs phenomenon. The main purpose of this paper is to show that high order accuracy can be recovered from spectral approximation contaminated with the Gibbs phenomenon if proper workarounds are applied. In this paper, we review some spectral method convergence remedies including spectral collocation grid stretching method (SCGSM), spectral collocation discontinuity inclusion method (SCDIM), and spectral collocation domain decomposition method (SCDDM) in pricing options. We first perform barycentric interpolations on European vanilla, bull spread, and butterfly option payoffs, solve numerically the Black Scholes partial differential equation (PDE) with the proposed workarounds of barycentric spectral methods and then perform numerical comparisons. In this paper, the SDDM appears to be the most accurate workaround when solving a Black Scholes PDE with different payoffs

Keywords: Spectral methods, Gibbs phenomenon, Grid stretching, Domain inclusion, Domain decomposition, Payoff, Financial options.

1 Introduction

The application and the investigation of spectral methods in interpolation and approximation theory [5,7,11], numerical integration [6,8,23], special function theory [16], and computational fluid dynamics are important in the study of orthogonal polynomials sequences. They are powerful tools to approximate functions that are difficult to compute and form part of the essential elements of numerical integration and approximation of solutions in differential, integral equations theories [26]. One can also consult [21,22] for the spectral method applications in quantum optics and electrical engineering.

Smooth functions are often approximated by using polynomial interpolations since they provide a strong and rapid convergence. However, for functions having discontinuities in the domain of interest, polynomial interpolants are unable to produce a high accuracy [17]. In the presence of such phenomenon the accuracy of high order methods deteriorates. This is due to the well-known Gibbs phenomenon that states that the pointwise convergence of global approximations of discontinuous functions is at most first order [12,20]. Thus, it is often perceived that spectral methods are too sensitive and lack robustness to allow the modelling of problems of realistic complexity. These, by nature, are often non-smooth.

It is well-known that option prices and their derivatives usually change dramatically near slope discontinuities of the payoff functions due to the Gibbs phenomena. The phenomenon affects the convergence and solution of financial PDEs. This explains why the application of spectral methods to the field of computational finance is still limited. Several workarounds exist and are commonly used to suppress or avoid the phenomenon and then restore the exponential accuracy of these methods [20]. These include filtering [25], Gegenbauer reconstruction [9], grid stretching [3], and domain decomposition [27,15] methods. The method, which is mostly accurate, should have the exact location of all discontinuities. Recently, the workarounds, with regained robustness, have received considerable attention in the field of finance, due to their effectiveness [18].

In this paper, we proposed other methodologies that contribute in restoring higher convergence of spectral methods and thus alleviate the Gibbs phenomenon in

[*] Corresponding author e-mail: pindzaedson@yahoo.fr

pricing options. These are SCGSM, SCDIM, and SCDDM. The methodologies are not entirely new, only the application, combination, and comparison of these methodologies are quite novel in the field of finance.

The paper is structured as follows. Section 2 describes the mathematical model of the problem in consideration. Section 3 reviews spectral collocation interpolation, in barycentric form, and its enhancements, i.e., SCGSM, SCDIM and SCDDM in pricing options. We apply these interpolation methods on the payoffs of European call, bull spread call, and butterfly spread options; and thereafter perform numerical experiments. Section 4 deals with the application of these methodologies in the financial options. Conclusions are drawn in Section 5.

2 Problem descriptions and applications

To calculate or estimate the fair value of an option, we use mathematical models. Under the assumption of the geometric Brownian motion (GBM),the asset price is given by

$$\frac{dS(t)}{S(t)} = \mu dt + \sigma dW(t), \tag{1}$$

where μ is the drift of the stock, σ is the volatility, and $W(t)$ is the standard Brownian motion (Wiener process). The stock dynamics lead to the following PDE, representing a standard European call and put option or simply a Black-Scholes (BS) PDE [4],

$$\frac{1}{2}\sigma^2 S^2(t)\frac{\partial^2 V}{\partial S^2} + rS(t)\frac{\partial V}{\partial S} + \frac{\partial V}{\partial t} - rV = 0 \tag{2}$$

where V represents the call or put option price, with certain final payoff at maturity, and (2) is valid if $S > 0$, $0 \leq t \leq T$. In both equations (1) and (2). The volatility σ, is one of the most important parameters. It is a statistical measure of the market's behaviour or the guarantee for the market to rise or fall within a period of time. Its computation is done by using the variance of the price or return. A high value of volatility in the market indicates that prices change rapidly in a short period of time.

The general boundary values condition of (2) are

$$\begin{cases} V(S,0) = V_0, \\ V(0,t) = f(t) \\ V(S,t)_{\lim_{S\to\infty}} = g(t). \end{cases} \tag{3}$$

The initial and boundary condition determine the type of financial option in consideration. For instance, a European call option gives the holder the right to exercise the option at maturity time T. To buy the underlying asset at maturity time T, it makes sense if the asset price is higher than the exercise price $(S > K)$, because one can buy the asset for K and sell it immediately on the market for S. If this is not the case, then the option is worthless. The payoff function of a European call option has one discontinuity in the first derivative and is given by

$$f(S) = \max(S-K, 0), \tag{4}$$

where S is the stock price and K is the strike price.

A bull spread is a neutral strategy that is a combination of two call options. There are two strike prices (two discontinuities in the first derivative of the payoff) involved in the payoff function of a bull spread option. The payoff function of a bull spread option is given by

$$g(S) = \max(S-K_1, 0) - \max(S-K_2, 0), \;\; K_1 < K_2, \tag{5}$$

where S is the stock price, and K_1 and K_2 are strike prices.

A butterfly spread is a neutral strategy that is a combination of a bull spread and a bear spread. It is a limited profit, limited risk options strategy. There are three strike prices (discontinuities) involved in a butterfly spread and it can be constructed using calls or puts. The payoff function of a butterfly spread option is expressed as

$$h(S) = \max(S-K_1, 0) - 2\max(S-K_2, 0) + \max(S-K_3, 0), \tag{6}$$

where $K_2 = (K_1 + K_3)/2$, S is the stock price, K_1, K_2 and K_3 are three distinct strike prices such that $0 < K_1 < K_2 < K_3$. Figure 2.1 shows the payoffs of a European call option, a bull spread call option, and a butterfly spread option. For all tests performed in this section, the parameters are chosen such that, $K = 50$ for the European call, $K_1 = 40$, $K_2 = 60$ for a bull spread call, and $K_1 = 30$, $K_2 = 50$, $K_3 = 70$ for a butterfly call option.

3 Numerical interpolations and applications

In practice, we are often confronted with situations where only a limited amount of data is accessible and it is necessary to estimate values between two consecutive data points. We can construct new points between known data points by interpolation or smoothing techniques. In finance, only a finite set of securities are traded in the financial markets, therefore it is very important to construct a sensible curve or surface from discrete observable quantities using interpolation methods.

In this section, we describe spectral methods used to interpolate the payoffs for European call, bull spread call, and butterfly spread options and we review SCGSM, SCDIM, and SCDDM in barycentric form.

To show the efficiency of present methods in comparison with the exact solution we report the maximum error which is defined by

$$L_\infty = ||u-U||_\infty = \max_{1\leqslant i\leqslant N} |u(x_i) - U(x_i)|, \tag{7}$$

where u and U represent the exact and approximate solutions, respectively. We refer by *error* the absolute value of the difference between the exact and the numerical solution.

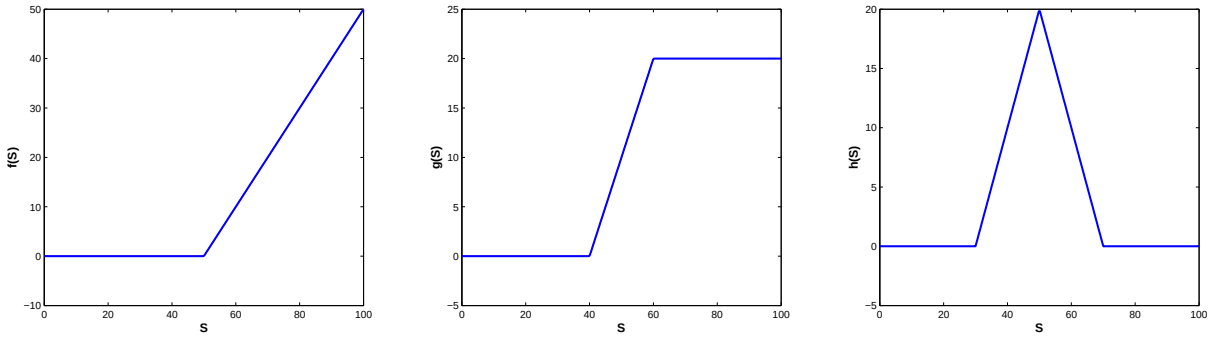

(a) European call option (b) Bull spread call option (c) Butterfly call option

Fig. 2.1: Payoff of a European call, bull spread call, and a butterfly call option. Left: $K = 50$. Middle: $K_1 = 40$ and $K_2 = 60$. Right: $K_1 = 30$, $K_2 = 50$, and $K_3 = 70$.

3.1 Spectral barycentric interpolation

The review done by [14] on the Lagrange interpolation and the barycentric formula shows the importance of discretisation in space with spectral methods. At first, a polynomial $u_N(x)$ is considered to be found among the vector space of all polynomials of degree N such that $u_N(x_j) = u_j$ with $j = 0,.....,N$. The result can be written in the Lagrange form as ([10])

$$u_N(x) = \sum_{j=0}^{N} u_j \gamma_j(x), \quad \gamma_j = \prod_{k=0,k\neq j}^{N} \frac{x - x_k}{x_j - x_k} \tag{8}$$

with the Lagrange polynomial γ_j corresponding to the node x_j with the property

$$\gamma_j(x_k) = \begin{cases} 1 \text{ when } & j = k \\ 0 \text{ otherwise} & \end{cases}. \tag{9}$$

The disadvantages of (8) are
1. The evaluation of each $u_N(x)$ needs an $\mathcal{O}(N^2)$ additions and multiplications.
2. The addition of a new pair of data (x_{N+1}, u_{N+1}) leads to a completely new computation.
3. The presence of instability in the numerical computation is certain.

For that reason, (8) requires modifications to overcome these disadvantages. Berrut and Trefethen [3] modified (8) such that $u_N(x)$ can be computed in $\mathcal{O}(N)$ operations. This yields the barycentric formula $u_N(x)$ as

$$u_N(x) = \frac{\sum_{j=0}^{N} \frac{w_j}{x - x_j} u_j}{\sum_{j=0}^{N} \frac{w_j}{x - x_j}}, \tag{10}$$

where $w_0, w_1, \ldots, w_N$ are called barycentric weights. For every set of points $\{x_k\}$, there is a unique set of barycentric weights $\{w_k\}$. In this paper, we only consider the Chebyshev points $x_k = cos(\frac{k\pi}{N})$, $k = 0,1,2,....,N.$, with a set of barycentric weights $w_0 = c/2$, $w_k = (-1)^k c, k = 1,\ldots,N-1$, and $w_N = (-1)^N c/2$ for some non-zero constant c [2]. More details are given in [3] to obtain (10).

The barycentric interpolation method is used to approximate the solutions of a differential equation by a polynomial which interpolates data $u_k = u(x_k)$ at the Chebyshev points $x_k = cos(\frac{k\pi}{N})$, $k = 0,1,2,....,N$. The data u_k must be determined by the polynomial interpolants that satisfy the differential equation exactly at the points x_k. Depending on the smoothness of the solution, the error will decline at a different rate as N increases [24].

To represent the payoff of a European call, a bull spread call, and a butterfly call option in the Chebyshev interpolation form, we transformed the Chebyshev domain $[-1,1]$ to a physical domain $[S_{min}, S_{max}]$. We use, without loss of generality, $S = \frac{1}{2}(S_{max} - S_{min})x + \frac{1}{2}(S_{max} + S_{min})$, where x is the Chebyshev point. The graphs in Figure 3.1 are obtained for $S_{min} = 0$, $S_{max} = 100$ and $N = 200$.

The *error* between the original payoff and the approximated Chebyshev interpolated payoff of the three call options is significantly lower, away from the jump discontinuity points (K, K_1, K_2, K_3) while it is very high at the discontinuity points. This confirms the problem of accuracy at these discontinuity points. To solve the problem of low accuracy at those points, one can use methods such as the grid stretching, discontinuity inclusion, or domain decomposition methods.

3.2 Grid stretching

In the most common barycentric pseudospectral methods, the interpolation points in the interval $[-1,1]$ are the Chebyshev collocation points y_k, $k = 0,\ldots,N$. The Chebyshev points are clustered near the boundaries of $[-1,1]$. However, we need to accumulate these points in the vicinity of the region of rapid change. One way to do

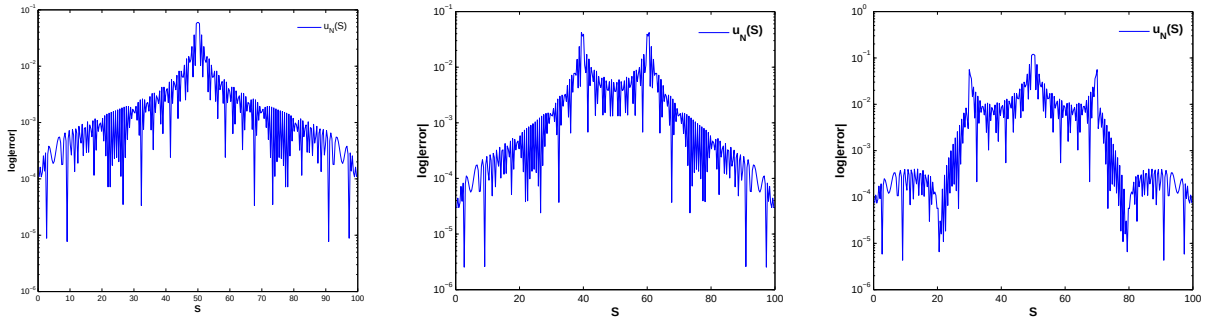

(a) European call option (b) Bull spread call option (c) Butterfly call option

Fig. 3.1: Corresponding L_2-Error between the numerical payoff and the Chebyshev interpolated payoff of a European call, bull spread call, and butterfly call option with $N = 200$.

this is to use adaptive grids via coordinate transformations. In Pindza *et al.* [14], to overcome the problem of discontinuity and differentiability in a payoff condition at a strike price, grid refinement is one of the best tools to retain a satisfactory accuracy of the spectral method applied on those payoffs. The local grid refinement is known to improve the accuracy of numerical methods. In this paper, we use the conformal map g given in Pindza *et al.* [14]

$$x = g(y) = \beta + \frac{1}{\alpha}\sinh\left[\bar{\lambda}(y-\mu)\right], \tag{11}$$

where

$$\bar{\lambda} = \frac{\gamma+\delta}{2}, \quad \mu = \frac{\gamma-\delta}{\gamma+\delta}, \tag{12}$$

with

$$\gamma = \sinh^{-1}[\alpha(1+\beta)], \quad \delta = \sinh^{-1}[\alpha(1-\beta)], \tag{13}$$

where α and β determine the location and the magnitude of the region of rapid change. The conformal map g is constructed from

$$y = g^{-1}(x) = \mu + \frac{1}{\lambda}\sinh^{-1}[\alpha(x-\delta)]. \tag{14}$$

A significant advantage of the rational collocation method based on rational interpolation in barycentric form is that tedious transformations using the chain rule to approximate the derivatives of u are not required, as it is usual in other spectral collocation methods.

The method shows a significant improvement of the approximation away from, and at the discontinuity points. As represented in Figure 3.2, the grid stretching method (SCGM) recovers the approximation very well at all levels. In all three cases, the error obtained using the SCGM is of magnitude 10^{-14}, as opposed to the error obtained using a naive spectral collocation method with an order of magnitude 10^{-2}.

3.3 Discontinuity inclusion

Often the computation of certain problems with jump discontinuity, involving piecewise analytic functions, can be performed easily. However, it is difficult to approximate functions with a single polynomial accurately. A higher order of accuracy can be achieved by modifying the spatial discretisation. A alternative is to use spectral discretisation based on the discontinuity inclusion approach. We divide the domain $\mathscr{D} = [a,b]$ into M sub-domains $\mathscr{D}_1 = (x^{(0)}, x^{(1)}), \mathscr{D}_2 = (x^{(1)}, x^{(2)}), ..., \mathscr{D}_M = (x^{(M-1)}, x^{(M)})$, where $x^{(0)} = a$ and $x^{(M)} = b$. The domain $\mathscr{D}$ is covered by M sub-domains as $\mathscr{D} = \bigcup_{\mu=1}^{M} \mathscr{D}_\mu$. The collocation points $x_j^{(n)}$ on $\mathscr{D}_n$ are defined by

$$x_k^{(n)} = \begin{cases} \frac{x^{(n)}-x^{(n-1)}}{2}\cos\left(\frac{k\pi}{N}\right) + \frac{x^{(n)}+x^{(n-1)}}{2}, 0 \leqslant k \leqslant N, \\ n = 1, \\ \frac{x^{(n)}-x^{(n-1)}}{2}\cos\left(\frac{k\pi}{N}\right) + \frac{x^{(n)}+x^{(n-1)}}{2}, 1 \leqslant k \leqslant N, \\ 2 \leqslant n \leqslant M. \end{cases} \tag{15}$$

The approximation of u uses the formula (10), where the barycentric weights $\{w_k\}$ are evaluated numerically. This strategy will cluster grid nodes not only at the boundaries located at S_{min} and S_{max}, but also at the singularity, which is located at the strike price for European options. This strategy is necessary to reduce the error caused by the non-smooth kink in the payoff function of most options. Note that this methodology is different from the domain decomposition method in the sense that the continuation condition is not needed here. In addition, all the matrices are full matrices, whereas in the case of the domain decomposition method the matrices are block diagonal matrices.

The approximation of the different call options is also improved at the discontinuity points when we use the grid stretching method, but the method does not give absolute accuracy for the solution. Figure 3.3 shows the superiority of this method over the use of the Chebyshev interpolation

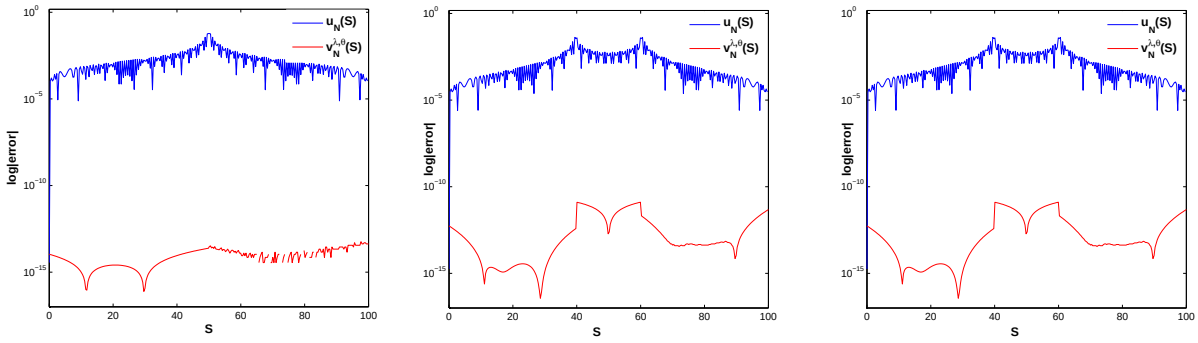

(a) European call options (b) Bull spread call options (c) Butterfly options

Fig. 3.2: Corresponding *error* between the original payoff and the interpolated payoff, by using the grid stretching method with $N = 200$ and $\alpha = 10^8$.

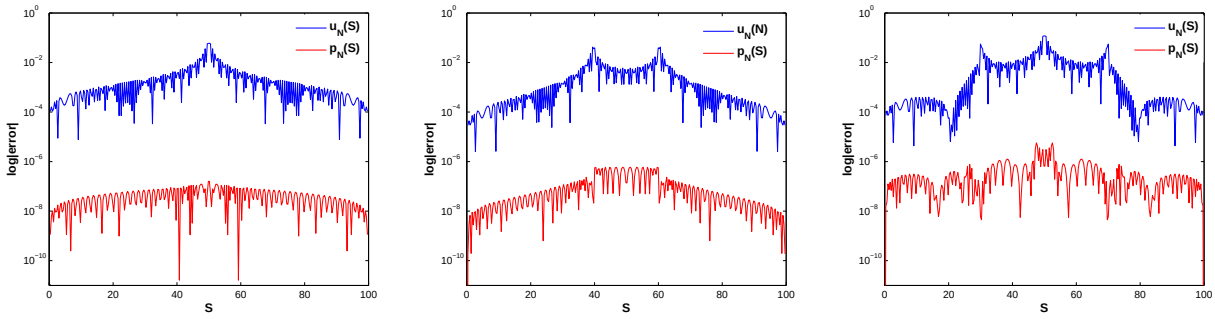

(a) European call options (b) Bull spread call options (c) Butterfly options

Fig. 3.3: Corresponding *error* between the original payoff and the interpolated payoff, using the discontinuity inclusion method with $N = 200$.

method. The method is 10^4 more accurate than the original Chebyshev method.

3.4 Domain decomposition

Challenges arise when we want to approximate a function with a jump discontinuity by using a high order spectral or finite difference methods. More often, the jumps and derivatives at discontinuity points of a function are known and the derivatives can be easily computed. However, it is difficult to accurately approximate a jump continuity in a function, or its derivatives, when we use a single polynomial. This is the case in option pricing problems.
To alleviate the problem, the use of some methods comes at a cost to accuracy near the discontinuities or in the computational cost, or in the implementation of the method. Nevertheless, a simple approach such as the spectral domain decomposition method can be used to recover the accuracy at discontinuity points [12].
The application is often done when the basis function is not continuous on the domain $\mathscr{D}$ [15].
Let $\mathscr{D} = [a,b]$, be broken into M sub-domains

$$\mathscr{D}_1 = (x^{(0)}, x^{(1)}), \mathscr{D}_2 = (x^{(1)}, x^{(2)}), ..., \mathscr{D}_M = (x^{(M-1)}, x^{(M)}),$$

with $x^{(0)} = a, x^{(M)} = b$. In general, $\mathscr{D}$ is covered by $N_{\mathscr{D}}$ sub-domains as

$$\mathscr{D} = \bigcup_{\mu=1}^{N_{\mathscr{D}}} \mathscr{D}_\mu, \tag{16}$$

where each sub-domains has its own set of basis functions and expansion coefficients

$$u^{(\mu)}(x) = \sum_{k=0}^{N_\mu} \tilde{u}_k^{(\mu)} \phi_k^{(\mu)}(x), \quad x \in \mathscr{D}_\mu, \quad \mu = 1, ...N_{\mathscr{D}} \tag{17}$$

The notation $u^{(\mu)}$ represents the approximation in the μth domain, and the different sub-domains $\mathscr{D}_\mu$ can touch or overlap each other. For example, solving a second order non-linear elliptic PDE or system of equation,

$$(\mathscr{N}u)(x) = 0, \quad x \in \mathscr{D}, \tag{18}$$

in the domain $\mathscr{D} \subset \mathbb{R}^d$ with boundary conditions

$$g(u)(x) = 0 \quad x \in \partial\mathscr{D},$$

where $\mathscr{N}$ and d denote the elliptic operator and mappings, the matching conditions must satisfy. Therefore, each functions $u^{(\mu)}$ defined only on the single sub-domain $\mathscr{D}_\mu$ must fit together to form a smooth solution of (18) over the full domain $\mathscr{D}$. For infinite resolution, the following conditions at the limit must hold [15]:

1. When two sub-domains, $\mathscr{D}_\mu$ and $\mathscr{D}_\nu$, touch each other on the intersection surface, the function and its derivative must be smooth, hence

$$\begin{cases} u^\mu(x) = u^\nu(x) \\ \frac{\partial u^\mu}{\partial n}(x) = -\frac{\partial u^\nu}{\partial n}(x) \\ \quad x \in \partial\mathscr{D}_\mu \cap \partial\mathscr{D}_\nu. \end{cases} \tag{19}$$

2. When two sub-domains, $\mathscr{D}_\mu$ and $\mathscr{D}_\nu$, overlap each other, the functions $u^{(\mu)}$ and $u^{(\nu)}$ must be identical in $\mathscr{D}_\mu \cap \mathscr{D}_\nu$. Since the solution of a PDE is unique, we must prove that, at the boundary of the overlapping domain,

$$u^{(\mu)}(x) = u^{(\nu)}(x) \quad x \in \partial(\mathscr{D}_\mu \cap \mathscr{D}_\nu). \tag{20}$$

An application of this approach on the different call options leads to the results obtained in Figure 3.4.

We compare the results obtained with the SCM to those of the SCDDM. The results are shown in Figure 3.4. In all the cases Figure 3.4 shows highly accurate results are obtained with the SCDDM, while poor accuracy in recorded with SCM. It is noted that for $N = 200$, the magnitude of absolute error is 10^{-14} for SCDDM and 10^{-2} for SCM. The SCDDM allows the removal of the Gibbs phenomenon and restores spectral accuracy for discontinuous problems.

Lastly, we investigate the numerical convergence of the interpolation methods used in this section. We vary the number of grid points and record the maximal error. All the results are shown is Figure 3.5. It can be observed that SCM has very poor convergence. Other methods detain a very fast convergence as compared to the SCM. The SCDDM shows the best convergence as the number of grid points are increased.

In the next section, we employ these methods to numerically solve the Black Scholes PDE.

4 Numerical discretisation and application

PDEs are commonly solved by using basic approaches such as finite difference, finite elements and spectral method. Among these methods, finite difference method appears to be the easiest to code. Since the method converges only algebraically, a large number of grid points and memory are needed. The other two approaches expand the solution of PDEs in basis functions. However, the difference is that finite element methods use many sub-domains and expand the solution to low order in each sub-domain. On the other hand, to obtain the solution to a PDE, the spectral method uses few sub-domains with high expansion orders compared to the finite elements approach. The method offers a fast convergence and accurate solution.

The work of the German mathematician, Hermann Schwarz, is one of the fundamental beginnings of the domain decomposition method (DDM). It was first designed to solve PDEs on parallel computers. The method solves boundary value problems by dividing the interval into smaller boundaries called sub-domains and recapitulates the solution between adjacent sub-domains. DDM offers several advantages in mathematics, as mention by [27].
Orszag [13] introduced the DDM in spectral method. His work produced the multi-domain spectral method which consists of matching the solution across different sub-domain.

In the next subsection, we show the space discretisation of Black Scholes PDE by means of the domain decomposition method. Note that the domain decomposition method is a generalisation of other methods discussed in this paper.

4.1 Space discretisation using the domain decomposition method

Suppose the domain $\mathscr{K} = [0, S_{\max}]$ of (2) is broken into M sub-domains $\mathscr{K}_1 = (S^{(0)}, S^{(1)}), \mathscr{K}_2 = (S^{(1)}, S^{(2)}), ..., \mathscr{K}_M = (S^{(M-1)}, S^{(M)})$, where $S^{(0)} = 0$ and $S^{(M)} = S_{\max}$. On the interval $\mathscr{K}$, the solution of (2) will be represented by V and on its decomposed domain $\tilde{\mathscr{K}}_n = [S^{n-1}, S^n]$ by V_n. All approximated solutions of $\mathscr{K}, \tilde{\mathscr{K}}$ will be represented by V^N and V_n^N. Meanwhile, the collocation points on $\mathscr{K}_n$ are denoted by $S_j^{(n)}, 0 \leqslant j \leqslant N, 1 \leqslant n \leqslant M$, with N as a known integer. Therefore, we denote $S_j^{(n)}$, $0 \leqslant j \leqslant N, 1 \leqslant n \leqslant M$, as

$$S_j^{(n)} = \frac{S^{(n)} - S^{(n-1)}}{2} \cos\left(\frac{j\pi}{N}\right) + \frac{S^{(n)} + S^{(n-1)}}{2}$$

,

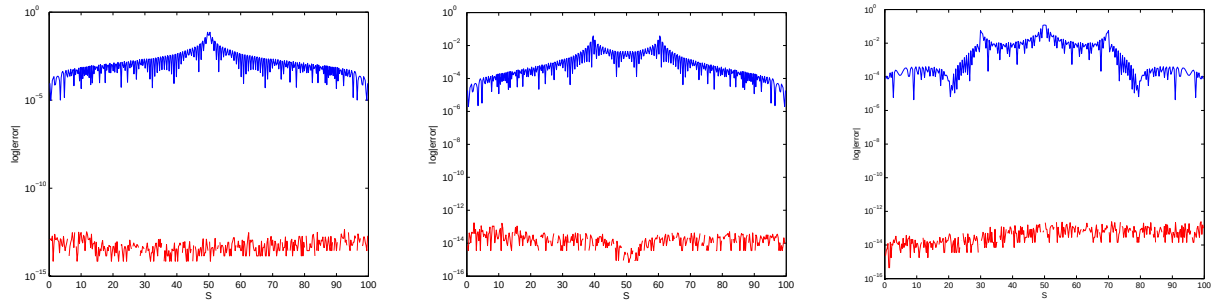

(a) European call options (b) Bull spread call options (c) Butterfly options

Fig. 3.4: Corresponding Log-Error when using the domain decomposition method on a European call ($\mu = 3$, $\mathscr{D}_1 = 0, \mathscr{D}_2 = 50, \mathscr{D}_3 = 100$), bull spread call ($\mu = 4$, $\mathscr{D}_1 = 0, \mathscr{D}_2 = 40, \mathscr{D}_3 = 60, \mathscr{D}_4 = 100$), and butterfly spread call ($\mu = 5$, $\mathscr{D}_1 = 0, \mathscr{D}_2 = 30, \mathscr{D}_3 = 50, \mathscr{D}_4 = 70, \mathscr{D}_5 = 100$) option with $N = 200$

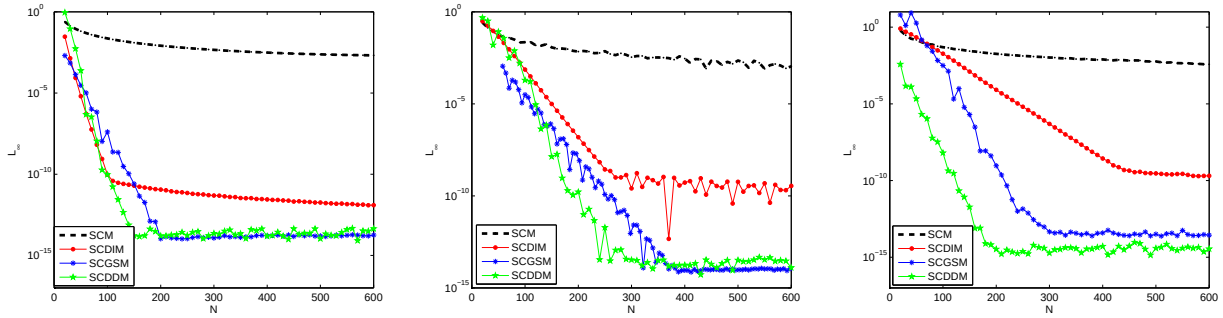

(a) European call option (b) Bull spread call option (c) Butterfly call option

Fig. 3.5: Numerical convergence of SCM, SCDIM,SCGSM and SCDDM

A patching method for the BS equation is written as

$$\begin{cases} \frac{\partial V_1^N}{\partial t}\Big|_{S=S_j^1} + \frac{1}{2}\sigma^2 S^2 \frac{\partial^2 V_1^N}{\partial S^2}\Big|_{S=S_j^1} + \\ \qquad rS\frac{\partial V_1^N}{\partial S}\Big|_{S=S_j^1} - rV_1^N\big|_{S=S_j^1} = 0 \\ \frac{\partial V_2^N}{\partial t}\Big|_{S=S_j^2} + \frac{1}{2}\sigma^2 S^2 \frac{\partial^2 V_2^N}{\partial S^2}\Big|_{S=S_j^2} + \\ \qquad rS\frac{\partial V_2^N}{\partial S}\Big|_{S=S_j^2} - rV_2^N\big|_{S=S_j^2} = 0 \\ \qquad\qquad \vdots \\ \frac{\partial V_M^N}{\partial t}\Big|_{S=S_j^M} + \frac{1}{2}\sigma^2 S^2 \frac{\partial^2 V_M^N}{\partial S^2}\Big|_{S=S_j^M} + \\ \qquad rS\frac{\partial V_M^N}{\partial S}\Big|_{S=S_j^M} - rV_M^N\big|_{S=S_j^M} = 0, \\ \qquad\qquad j = 0:N, \end{cases} \tag{21}$$

with the boundary conditions

$$\begin{aligned} V_{n-1}^N\left(S^{(n-1)},t\right) &= V_n^N\left(S^{(n-1)},t\right),\ n = 2:M, \\ \frac{\partial V_{n-1}^N}{\partial S}\left(S^{(n-1)},t\right) &= \frac{\partial V_n^N}{\partial S}\left(S^{(n-1)},t\right),\ n = 2:M, \\ V_{n-1}^N(S^{(0)},t) &= f(t) \\ V_{n-1}^N(S^{(M)},t) &= g(t) \end{aligned}$$

To discretise Equation (21) in space, we replace $\frac{\partial V_i^N}{\partial S}\Big|_{S=S_j^i}$ and $\frac{\partial^2 V_i^N}{\partial S^2}\Big|_{S=S_j^i}$ by the following pseudo-spectral approximations

$$\frac{\partial V_i^N}{\partial S}\Big|_{S=S_j^i} = 2\frac{\sum_{p=0}^N D_{jp}^{(m)}\left(V_i^N(S_p^{(i)},t) - V_i^N(S_j^{(i)},t)\right)}{S^{(i)} - S^{(i-1)}}, \quad p = 1,\ldots,N-1 \tag{22}$$

and

$$\left.\frac{\partial^2 V_i^N}{\partial S^2}\right|_{S=S_j^i} = 4\frac{\sum_{p=0}^{N} D_{jp}^{(m)}\left(V_i^N(S_p^{(i)},t) - V_i^N(S_j^{(i)},t)\right)}{\left(S^{(i)}-S^{(i-1)}\right)^2}, \quad p = 1,...,N-1 \tag{23}$$

where $D_{jp}^{(m)}$ are the entries of the differentiation matrix of order $m = 1,2$.
By setting

$$U_{ip}^N(t) = V_i^N(S_p^{(i)},t), U_{1N}^N(t) = f(t), U_{M0}^N(t) = g(t)$$

and substituting (22), (23) into (21) we get

$$\begin{array}{c} \frac{dU_{1j}^N(t)}{dt} + \mathscr{W}_1 = 0, \\ \frac{dU_{2j}^N(t)}{dt} + \mathscr{W}_2 = 0, \\ \vdots \\ \frac{dU_{Mj}^N(t)}{dt} + \mathscr{W}_M = 0 \end{array} \tag{24}$$

where

$$\left\{\begin{array}{l} \mathscr{W}_1 = \frac{2\sigma^2 S^2}{\left(S^{(1)}-S^{(0)}\right)^2}\sum_{p=0}^{N} D_{jp}^2\left(U_{1p}^N(t) - U_{1j}^N(t)\right) + \\ \frac{2rS}{\left(S^{(1)}-S^{(0)}\right)^2}\sum_{p=0}^{N} D_{jp}\left(U_{1p}^N(t) - U_{1j}^N(t)\right) - rU_{1j}^N(t) \\ \mathscr{W}_2 = \frac{2\sigma^2 S^2}{\left(S^{(2)}-S^{(1)}\right)^2}\sum_{p=0}^{N} D_{jp}^2\left(U_{2p}^N(t) - U_{2j}^N(t)\right) + \\ \frac{2rS}{\left(S^{(2)}-S^{(1)}\right)^2}\sum_{p=0}^{N} D_{jp}\left(U_{2p}^N(t) - U_{2j}^N(t)\right) - rU_{2j}^N(t) \\ \vdots \\ \mathscr{W}_M = 2\sigma^2 S^2\left(S^{(M)}-S^{(M-1)}\right)^{-2}\sum_{p=0}^{N} D_{jp}^2\mathscr{U} + \beta, \end{array}\right. \tag{25}$$

with

$$\mathscr{U} = \left(U_{Mp}^N(t) - U_{Mj}^N(t)\right),$$

$$\beta = 2rS\left(S^{(M)}-S^{(M-1)}\right)^{-2}\sum_{p=0}^{N} D_{jp}\mathscr{U} - rU_{Mj}^N(t),$$

and

$$\begin{array}{c} U_{10}^N(t) = U_{2N}^N(t), \\ U_{20}^N(t) = U_{3N}^N(t), \\ \vdots \\ U_{M-1,0}^N(t) = U_{MN}^N(t), \\ U_{1N}^N(t) = f(t), \ \ U_{M0}^N(t) = g(t). \end{array} \tag{26}$$

$$\begin{array}{c} \frac{\partial V_1^N}{\partial S}\left(S_0^{(1)},t\right) = \frac{\partial V_2^N}{\partial S}\left(S_N^{(2)},t\right), \\ \frac{\partial V_2^N}{\partial S}\left(S_0^{(2)},t\right) = \frac{\partial V_3^N}{\partial S}\left(S_N^{(3)},t\right), \\ \vdots \\ \frac{\partial V_{M-1}^N}{\partial S}\left(S_0^{(M-1)},t\right) = \frac{\partial V_M^N}{\partial S}\left(S_N^{(M)},t\right). \end{array} \tag{27}$$

Equations (26) and (27) can be approximated by using (22) and (23) as

$$\begin{array}{c} \left(\frac{2}{S^{(1)}-S^{(0)}}\right)\sum_{p=0}^{N} D_{0p}^{(m)}\left(U_{1p}^N(t) - U_{10}^N(t)\right) = \mathscr{A}, \\ \left(\frac{2}{S^{(2)}-S^{(2)}}\right)\sum_{p=0}^{N} D_{0p}^{(m)}\left(U_{2p}^N(t) - U_{20}^N(t)\right) = \mathscr{B}, \\ \vdots \\ \left(\frac{2}{S^{(M-1)}-S^{(M-2)}}\right)\sum_{p=0}^{N} D_{0p}^{(m)}\left(U_{M-1,p}^N(t) - U_{M-1,0}^N(t)\right) = \mathscr{C}, \end{array} \tag{28}$$

with

$$\mathscr{A} = \left(\frac{2}{S^{(2)}-S^{(1)}}\right)\sum_{p=0}^{N} D_{Np}^{(m)}\left(U_{2p}^N(t) - U_{2N}^N(t)\right),$$

$$\mathscr{B} = \left(\frac{2}{S^{(3)}-S^{(2)}}\right)\sum_{p=0}^{N} D_{Np}^{(m)}\left(U_{3p}^N(t) - U_{3N}^N(t)\right)$$

and

$$\mathscr{C} = \left(\frac{2}{S^{(M)}-S^{(M-1)}}\right)\sum_{p=0}^{N} D_{Np}^{(m)}\left(U_{Mp}^N(t) - U_{MN}^N(t)\right).$$

Therefore Equation (24) and (28) can be rewritten as a system of differential algebric equations (DAEs) of the form,

$$\left\{\begin{array}{l} Y'(t) = F(t,Y(t)), \\ Q_1(t,Y(t)) = 0, \\ Q_2(t,Y(t)) = 0, \\ Q_3(t,Y(t)) = 0, \\ Y(0) = Y_0, \end{array}\right. \tag{29}$$

with

$$Y(t) = [U_{10}^N(t), U_{11}^N(t), ..., U_{1N}^N(t), ..., U_{M0}^N(t), ..., U_{MN}^N(t)]^T,$$

$$Y_0 = [V_0(S_0^1), V_0(S_1^1), ..., V_0(S_N^1), ..., V_0(S_0^M), ..., V_0(S_N^M)]^T,$$

$$Y'(t) = [U_{10}^{N'}(t), U_{11}^{N'}(t), ..., U_{1N}^{N'}(t), ..., U_{M0}^{N'}(t), ..., U_{MN}^{N'}(t)]^T$$

$$F(t,Y(t)) = [F_{ij}(t,Y(t))]_{\{M\times(N+1)\}\times\{M\times(N+1)\}},$$

$$Q_1(t,Y(t)) = [Q_{11}(t,Y(t)), ..., Q_{1,M-1}(t,Y(t))],$$

$$Q_2(t,Y(t)) = [Q_{21}(t,Y(t)), ..., Q_{2,M-1}(t,Y(t))],$$

$$Q_3(t,Y(t)) = [Q_{31}(t,Y(t)), ..., Q_{3,2}(t,Y(t))],$$

and

$$F_{ij}(t,Y(t)) = -\Omega + rU_{ij}^N(t)$$

$$\Omega = \frac{2\sigma^2 S^2}{\left(S^{(i)}-S^{(i-1)}\right)^2}\sum_{p=0}^{N} D_{jp}^2\left(U_{ip}^N(t) - U_{ij}^N(t)\right) + \mathscr{E},$$

$$\mathscr{E} = \frac{2rS}{\left(S^{(1)}-S^{(0)}\right)^2}\sum_{p=0}^{N} D_{jp}\left(U_{ip}^N(t) - U_{ij}^N(t)\right),$$

$$Q_{1,i}(t,Y(t)) = [U_{i0}^N(t) - U_{i+1,N}^N(t)],$$

$$Q_{2,i}(t,Y(t)) = \sum_{p=0}^{N}(\alpha_1, -\alpha_2),$$

$$\alpha_1 = 2\left(S^{(i)} - S^{(i-1)}\right)^{-2} D_{0p}\left(U^N_{ip}(t) - U^N_{i0}(t)\right),$$

$$\alpha_2 = 2\left(S^{(i+1)} - S^{(i)}\right)^{-2} D_{Np}\left(U^N_{i+1,p}(t) - U^N_{i+1,N}(t)\right),$$

$$Q_{3,1}(t,Y(t)) = U^N_{0N}(t) - f(t),$$

$$Q_{3,2}(t,Y(t)) = U^N_{M0}(t) - g(t).$$

The above discretisation (29) leads to the semi-discrete linear system

$$Y' = AY + b(t), \;\; b(t) = \varepsilon_1 + \varepsilon_2 e^{-rt}, \tag{30}$$

where A is either a block dense diagonal matrix or a dense matrix depending on the number of domains in consideration. The parameters ε_1 and ε_2 are given by the boundary conditions.

4.2 Exponential time differencing schemes

The above discretisation (29) leads to the semi-discrete linear system

$$Y' = AY + b(t), \;\; b(t) = \varepsilon_1 + \varepsilon_2 e^{-rt}, \tag{31}$$

where A is either a block dense diagonal matrix or a dense matrix depending on the number of domains in consideration. The parameters ε_1 and ε_2 are given by the boundary conditions. Integrating the system of ODE (31) on the interval $[0\ T]$ leads to the scheme

$$\begin{aligned} Y(T) &= e^{AT}Y(0) + e^{AT}\int_0^T e^{-At}b(t)dt \\ &= e^{AT}Y(0) + \mathscr{G} \end{aligned}$$

where

$$\mathscr{G} = A^{-1}\left(e^{AT} - I\right)\varepsilon_1 - (A - rI)^{-1}\left(e^{AT} - e^{-rT}I\right)\varepsilon_2,$$

and I is the identity matrix. Note that computation of the price of European options using (32) requires forming the matrix functions $f_1(A) = e^{AT}$, $f_2(A) = A^{-1}\left(e^{AT} - I\right)$ and $f_3(A) = (A - rI)^{-1}\left(e^{AT} - e^{-rT}I\right)$. In order to overcome the numerical difficulties encountered in computing matrix functions, we employ the Krylov projection algorithm [19]. The key idea behind this method is to approximate the product of a matrix function $\varphi(A)$ (A is a $N \times N$ matrix) and a vector v, using projection of the matrix and the vector onto the Krylov subspace $K_m(A,v) = span\{v, Av, \ldots, A^{m-1}v\}$. The orthonormal basis $\{v_1, v_2, \ldots, v_m\}$ of $K_m(A,v)$ is constructed using the modified Arnoldi iteration [1,19] which can be written in matrix form as

$$AV_m = V_m H_m + \bar{h}_{m+1,m} v_{m+1} e_m^T, \tag{32}$$

where $\bar{h}_{m+1,m}$ is an entry of the Hessenberg matrix H_m, $e_m = (0,\ldots,0,1,0,\ldots,0)^T$ is the unit vector with 1 as the m^{th} coordinate, $\{v_1, v_2, \ldots, v_m, v_{m+1}\}$ is an orthonormal basis of $K_m(A,b)$, $V_m = [v_1 v_2 \ldots v_m] \in \mathbb{R}^{N\times m}$, and

$$H_m = V_m^T A V_m, \tag{33}$$

is an upper Hessenberg matrix calculated as a side product of the iteration. Matrix $P = V_m V_m^T$ is a projector onto $K_m(A,v)$, thus $\varphi(A)v$ is approximated as a projection

$$\varphi(A)b \approx V_m V_m^T \varphi(A) V_m V_m^T b. \tag{34}$$

Recalling (33) and observing that $v_1 = v/\|v\|_2$, we make the final approximation through

$$\varphi(A)v \approx \|v\|_2 V_m \varphi(H_m) e_1. \tag{35}$$

The advantage of this formulation is that H_m is a $m \times m$ matrix of smaller size $(m \ll N)$ and and is therefore much cheaper to evaluate $\varphi(H_m)$ than $\varphi(A)$.

4.3 Numerical results

We apply the spectral approximation methods to value the Black Scholes PDE (2) using the SCM, SCGSM, SCDIM, and SCDDM. We use three different payoffs, namelly a European call (4) and bull spread (5) and butterfly spread (6) options. Hence, boundary value conditions are expressed as, for a European call option

$$V(0,t) = 0, \;\text{ and }\; V(S_{\max},t) = S_{\max} - Ke^{-rt}. \tag{36}$$

For a European bull spread call option we have

$$V(0,t) = 0, \;\text{ and }\; V(S_{\max},t) = S_{\max} - (K_2 - K_1)\,e^{-rt}, \tag{37}$$

with $K_1 < K_2$.
For a European butterfly spread call option

$$V(0,t) = 0, \;\text{ and }\; V(S_{\max},t) = 0, \;\; K_1 < K_2 < K_3. \tag{38}$$

We solve the PDE (2) using the parameters $r = 0.05$, $\sigma = 0.2$, $K = 50$, $S_{\min} = 0$, $S_{\max} = 4K$ for a European call option (36), $r = 0.05$, $\sigma = 0.2$, $K_1 = 60$, $K_2 = 80$ $S_{\min} = 0$, $S_{\max} = 4K_1$ for a European bull spread call option (37), and $r = 0.05$, $\sigma = 0.2$, $K_1 = 90$, $K_2 = (K_1 + K_3)/2$, $K_3 = 110$, $S_{\min} = 0$, $S_{\max} = 4K_1$ for a European butterfly spread call option (38). In each case, the number of grid points is chosen to be $N = 100$.

We display the numerical and analytical solutions for the above mentioned options in Figure 4.1. The numerical solutions are in good agreement with the analytical ones. However, we only show numerical results obtained with the domain decomposition method for clarity. Although numerical solutions are in good agreement with the analytical solutions, we would like to investigate how close these solutions are. We plot the absolute difference between numerical and analytical solutions in Figure 4.2. To avoid a huge truncation error, we use $S_{\max} = 4K$ for

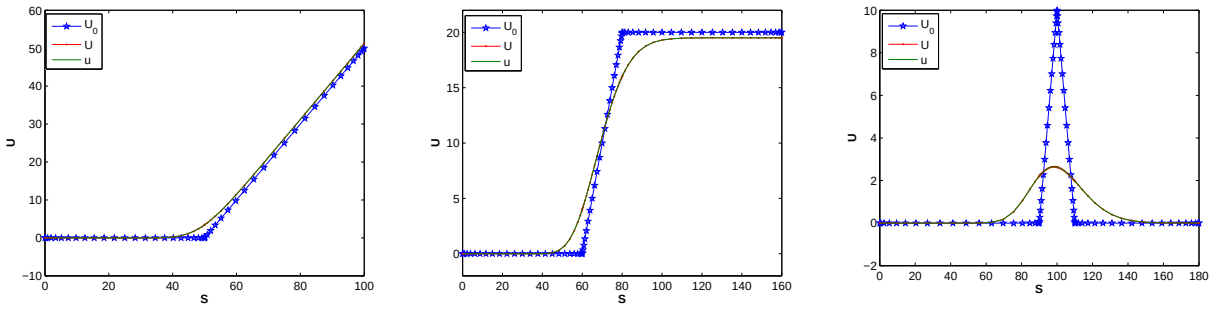

(a) European call option (b) Bull spread call option (c) Butterfly call option

Fig. 4.1: Solution errors between the analytical and numerical solutions obtained using SCM, SCGSM, SCDIM, and SCDDM with $N = 100, r = 0.05, T = 0.5, \sigma = 0.2, S_{\max} = 200, S_{\min} = 0$ for all options, $K = 50$ for a European call, $K_1 = 30, K_2 = 70$ for a bull spread call and $K_1 = 30, K_2 = 50, K_3 = 70$ for a butterfly call option.

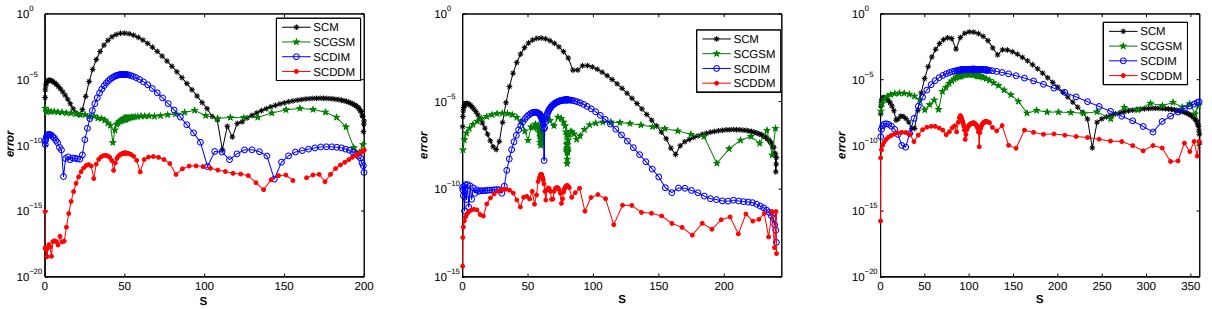

(a) European call option (b) Bull spread call option (c) Butterfly call option

Fig. 4.2: Solutions of the Black Scholes equation under SMBS with $N = 150, r = 0.05, T = 0.5, \sigma = 0.2, S_{\max} = 200, S_{\min} = 0$ for all options, $K = 50$ for European call, $K_1 = 30, K_2 = 70$ for a bull spread call and $K_1 = 30, K_2 = 50, K_3 = 70$ for a butterfly call option.

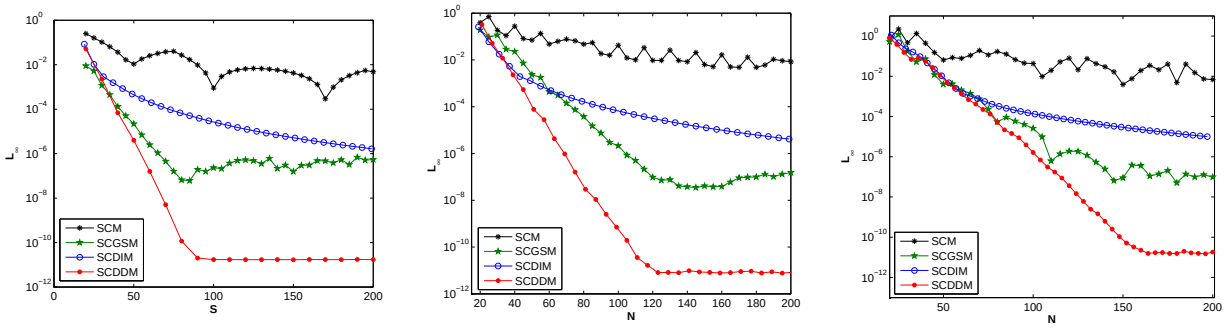

(a) European call option (b) Bull spread call option (c) Butterfly call option

Fig. 4.3: Numerical convergence of SCM, SCDIM,SCGSM and SCDDM with $N = 150, r = 0.05, T = 0.5, \sigma = 0.2, S_{\max} = 200, S_{\min} = 0, \alpha = 10^4$ for all options, $K = 50$ for European call, $K_1 = 30, K_2 = 70$ for a bull spread call and $K_1 = 30, K_2 = 50, K_3 = 70$ for a butterfly call option.

call options and $S_{\max} = 4K_1$ for bull and butterfly spread options. For the SCGSM, an additional parameter, the grid stretching parameter, was chosen such that $\beta = 10^4$. It is observed that the SCDDM has the smallest error of magnitude 10^{-11}, followed by the SCGSM with an error of magnitude 10^{-8}, the SCDIM with an error of magnitude 10^{-5} and finally SCM with an error of magnitude 10^{-2}.

In the last experiment, we investigate numerical convergence on these methods. We record the values of the maximal error while varying the number of grid points N. The results are shown in Figure 4.3. In each case, one can observe that the SCDDM detains the best convergence compared to the other methods. The convergence rate is exponential. The second best convergence is achieved by the SCGSM. This convergence depends on the choice of the grid stretching parameter β. One can use this parameter adaptively in order to achieve exponential convergence [14]. The SCDIM is the third best performing method. This method only improves the convergence of the spectral method without achieving exponential convergence. The SCM has a very bad convergence due to the Gibbs phenomenon at strike prices. In the presence of such a phenomenon, the accuracy of high order methods deteriorates [12, 20].

5 Conclusion

In this paper, we proposed a number of techniques to remove the Gibbs phenomenon encountered in interpolating non-smooth functions with spectral methods. We shown that high order accuracy can be recovered from spectral approximation contaminated with the Gibbs phenomenon if proper workarounds are applied. These include grid stretching (SCGM), discontinuity inclusion (SCDIM), and domain decomposition (SCDDM) methods in pricing options. Numerical tests are performed on a European vanilla, bull spread and butterfly option payoffs shown that the SCGSM, SCDIM, and SCDDM provide an efficient way to remove the Gibbs phenomenon. In the case of the SCDDM, the exponential convergence was achieved in pricing financial options. We are currently testing the performance of these techniques on Levy models for financial derivatives.

Acknowledgement

E. Pindza and F. Youbi are thankful to Brad Welch for the financial support through RidgeCape Capital.

References

[1] W. Arnoldi, The principle of minimized iteration in the solution of the matrix eigenvalue problem, *Quarterly of Applied Mathematics*, **9** (1951) 17-29.

[2] R. Baltensperger, J. P. Berrut, and B. Noël, Exponential convergence of a linear rational interpolant between transformed Chebyshev points, *Mathematics of Computation*, **68** (1999) 1109-1120.

[3] J. P. Berrut and L. N. Trefethen, Barycentric Lagrange Interpolation, *SIAM Review*, **46 (3)**, (2004) 501-517.

[4] T. Björk, *Arbitrage theory in continuous time*, 3rd edition, Oxford Finance University Press, New York, (2009).

[5] E. W. Cheney, *Introduction to Approximation Theory*, McGraw-Hill, New York, (1966).

[6] G. Dahlquist and A. Björck, *Numerical Methods in Scientific Computing*, Volume I. SIAM, Philadelphia, (2007).

[7] P. J. Davis, *Interpolation and Approximation*, Dover Publications Inc., New York, (1975).

[8] P. J. Davis and P. Rabinowitz, *Methods of Numerical Integration*, Second Edition, Academic Press, (1984).

[9] D. Gottlieb and C. -W. Shu, On the Gibbs phenomenon IV: Recovering exponential accuracy in a subinterval from a Gegenbauer partial sum of a piecewise analytic function, *Journal of Computational and Applied Mathematics*, **64** (1995) 1081-1095.

[10] J. L. Lagrange, Leçons élémentaires sur les mathématiques, *données à l'Ecole Normal en 1795, in Oeuvres VII, Gauthier-Villars, Paris*, **7** (1877) 183-287.

[11] J. C. Mason and D. C. Handscomb, *Chebyshev Polynomial*, CRC Press, New York, (2003).

[12] C. Markakis, and L. Barack, High-order difference and pseudospectral methods for discontinuous problems, *arXiv: 1406.4865v1 [maths.NA]*, (2014) 1-9.

[13] S. A. Orszag, Spectral methods for problems in complex geometries, *Journal of Computational Physics*, 37(1) (1980) 37-70.

[14] E. Pindza, K. C. Patidar and E. Ngounda, Implicit-Explicit Predictor-Corrector Methods Combined With Improved Spectral Methods For Pricing European Style Vanilla And Exotic Options, *Electronic Transaction on Numerical Analysis*, **40** (2013), 268-293.

[15] H. P. Pfeiffer, L. E. Kidder, M. A. Scheel, and S. A. Teukolsky, A multidomain spectral method for solving elliptic equations, *Computer Physics Communications* **152** (2003), 253-273.

[16] E. D. Rainville, *Special Functions*, Macmillan, New York, (1960).

[17] M. Richardson, *Chebyshev interpolation for functions with endpoint singularities via exponential and double-exponential transforms*, Oxford University, Mathematical Institute, UK, (2012).

[18] M. J. Ruijter, M. Versteegh, C. W. Oosterlee, On the application of spectral filters in a Fourier option pricing technique, *Journal of Computational Finance*, **19(1)** (2015) 1-24 .

[19] Y. Saad, *Iterative Methods for Sparse Linear Systems*, PWS Publishing Company, USA, 1996.

[20] S. A. Sarra, *Algorithm: The Matlab Postprocessing Toolkit*, ACM Transaction on Mathematical Software, Marshall University, Huntington, (2009).

[21] I. SenGupta, Spectral analysis for a three-dimensional superradiance problem, *Journal of Mathematical Analysis and Applications*, **375** (2011) 762-776.

[22] I. SenGupta *et al*, Concentration problems for bandpass filters in communication theory over disjoint frequency

intervals and numerical solutions, *Journal of Fourier Analysis and Applications*, **18** (2012) 182-210.
[23] E. Süli and D. Mayers, *An Introduction to Numerical Analysis*, Cambridge University Press, (2003).
[24] T. W. Tee, and L. N. Treffethen, A rational spectral collocation method with adaptively transformed Chebyshev grid points, *Journal of Scientific Computation* **28(5)** (2006) 1798-1811.
[25] H. Vandeven, Family of Spectral Filters for Discontinuous Problems, *SIAM Journal of Scientific Computing*, **6 (2)** (1991) 159-192.
[26] H. Wang and S. Xiang, On The Convergence Rates Of Legendre Approximation, *Mathematics Of Computation*, **81 (278)** (2012) 861-877.
[27] X. Wu and Y. Shen, Differential Domain Decomposition Method for a Class of Parabolic Equation, *Computer and Mathematics with Applications* **48** (2004) 1819-1832.

Francis Youbi is an MSc student in Financial Engineering at the department of Mathematics and Applied Mathematics at the University of Pretoria, South Africa. He is currently an Assistant Lecturer at the University of Pretoria. He is assisting the honours students with Financial Engineering courses and the first year students with Calculus topics. His research interest is in Financial Engineering.

Edson Pindza holds a PhD in computional finance. He was a quantitave analyst consultant at the Johannesburg Stock Exchange, a business analyst consultant at the South African Reserve Bank and a research associate in real options in the department of statistics and acturial sciences at the University of Western Ontario in Canada. He is currently an extraordinary lecturer in the Department of Mathematics and Applied Mathematics at the University of Pretoria and the founder of Crypto-Academy, an institution that provides training, consulting and educational programs in the field of cryptocurrency for various individual and organisational needs. His current research interest includes differential games in competitive Bitcoin mining rewards and financial derivatives in cryptocurrency ecosystems.

Eben Mare is responsible for Fixed Income at ABSA asset management. He has held senior positions in treasury trading and asset management over the last 25 years, including responsibility for absolute return investments at Stanlib asset management and head of market risk at ABSA Capital and Treasurer at Nedcor Investment Bank. He holds a Ph.D. in Applied Mathematics and a position as Associate Professor in the Department of Mathematics and Applied Mathematics at the University of Pretoria. He holds research interests in numerical analysis, derivatives pricing, and fund management.